ACS Medicinal Chemistry Letters

Letter

pubs.acs.org/acsmedchemlett

Missing Fragments: Detecting Cooperative Binding in Fragment-Based Drug Design

Pramod C. Nair,[†] Alpeshkumar K. Malde,[†] Nyssa Drinkwater,[‡,§] and Alan E. Mark*[,†,‡]

[†]School of Chemistry and Molecular Biosciences (SCMB) and [‡]Institute for Molecular Bioscience (IMB), The University of Queensland (UQ), St Lucia Campus, Brisbane, QLD 4072, Australia

[§]Randall Division of Cell and Molecular Biophysics, King's College London, London, SE1 1UL, United Kingdom

Supporting Information

ABSTRACT: The aim of fragment-based drug design (FBDD) is to identify molecular fragments that bind to alternate subsites within a given binding pocket leading to cooperative binding when linked. In this study, the binding of fragments to human phenylethanolamine *N*-methyltransferase is used to illustrate how (a) current protocols may fail to detect fragments that bind cooperatively, (b) theoretical approaches can be used to validate potential hits, and (c) apparent false positives obtained when screening against cocktails of fragments may in fact indicate promising leads.

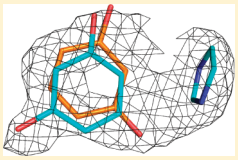

KEYWORDS: *molecular dynamics, drug binding, molecular fragments, free energy calculations, phenylethanolamine N-methyltransferase (PNMT)*

Fragment-based drug design (FBDD) is used increasingly in rational drug design. In fragment-based approaches, libraries of small molecules (50−250 Da) are screened against a specific protein target to identify fragments with high-quality interactions. The aim is to identify fragments that bind cooperatively and could be linked chemically to form potential lead molecules.[1] FBDD has been used to identify highly selective and potent inhibitors for various targets.[2−4] The potential of FBDD for the rapid identification and optimization of compounds is reflected in the number of molecules currently entering clinical trials.[5−8] A wide range of biophysical techniques including nuclear magnetic resonance, surface plasmon resonance, affinity mass spectrometry, etc. can in principle be used to identify which fragments bind to the target of interest. This said X-ray crystallography remains the method of choice in FBDD, as it can be used not only to identify fragments but more importantly to determine the mode of binding.

To achieve high throughput when using X-ray crystallography, fragments are normally screened as cocktails or mixtures. These cocktails are normally designed such that the fragments are chemically diverse and vary in size and shape so that a specific fragment might be identified based on its electron density alone. In cases where it is not possible to identify the fragment based on the electron density alone, the cocktails can be deconvoluted. That is, each fragment can be soaked individually into the crystal. Alternatively, complementary techniques such as mass spectroscopy or isothermal titration calorimetry (ITC) can also be used to confirm a proposed hit. One difficulty in using fragment-based approaches is that individual fragments often bind only weakly and techniques used to identify fragments are often applied at the limit of their sensitivity. In some cases, it is not possible to deconvolute a specific cocktail; in others, the binding of fragments identified crystallographically may not be confirmed using other techniques.

The type of challenges encountered when using FBDD approaches has been illustrated in a recent study by Drinkwater et al.[9] In this study, 96 cocktails containing in total 384 fragments were screened against human phenylethanolamine *N*-methyltransferase (hPNMT). PNMT catalyzes the conversion of *R*-noradrenaline to *R*-adrenaline in the presence of the cofactor *S*-adenosyl-L-methionine (Figure 1). Central nervous system-specific PNMT inhibitors are of potential therapeutic importance in Alzheimer's and Parkinson's disease.

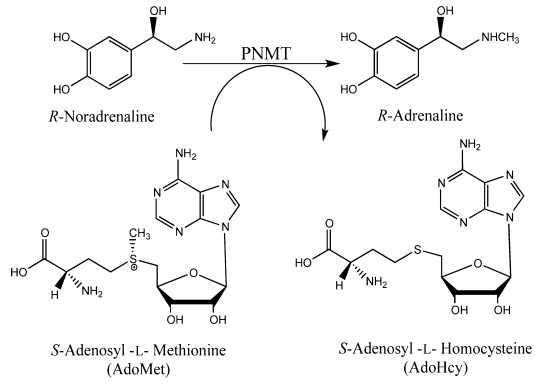

Figure 1. Schematic of the reaction catalyzed by PNMT involving transfer of a methyl group from AdoMet to noradrenaline, forming adrenaline and AdoHcy.

Of the 96 cocktails screened by Drinkwater et al.,[9] two caused crystal cracking. Of the remaining 94, 15 (16%) showed an apparent hit during the initial X-ray screens. Each of these cocktails contained four fragments. From these 60 fragments, 12,

Received: January 13, 2012
Accepted: February 14, 2012
Published: February 14, 2012

all binding in the same location, were ultimately identified based on X-ray crystallography (two from a single cocktail). Four of the 15 cocktails (27%) were considered to be false positives. A cocktail was considered to be a false positive if a specific fragment could not be identified based on the density alone, and no electron density was observed when the fragments were soaked individually into the crystal. To verify that the 12 fragments identified crystallographically were true hits, the affinity of these compounds for hPNMT was examined using ITC. Nine of the 12 fragments could be confirmed. Three of the 12 (25%) were below the detection limit.

Drinkwater et al.[9] also examined each member of three cocktails using electron spray ionization Fourier transform mass spectrometry (ESI-FTMS). These three cocktails collectively contained four fragments identified by X-ray crystallography. The binding of these four compounds could be verified by ESI-FTMS. Surprisingly, two additional fragments not detected by X-ray crystallography were shown to bind by ESI-FTMS.

There are multiple reasons why binding might be detected using a cocktail but not when fragments are examined individually. There are also many reasons why binding may be detected using one technique but not another. For example, different experimental conditions may be used. The average density observed in an X-ray diffraction experiment may result from multiple molecules occupying the same position in the crystal lattice or a given molecule adopting multiple positions. Alternatively, more than one fragment may bind cooperatively.

The primary aim of FBDD is to identify fragments that may be linked to generate potential lead compounds. Thus, identifying (a) how specific fragments bind within a given site and (b) which combinations of fragments can be accommodated simultaneously within the target are critical. We therefore investigated whether theoretical approaches, specifically, molecular dynamics (MD) simulations and free energy (FE) calculations, could be used to validate the binding mode of specific fragments to the noradrenaline binding pocket of hPNMT.[10]

As an initial step, the stability of the binding mode of the 12 fragments identified by X-ray crystallography (Table S1 in the Supporting Information) was examined. A series of simulations (each 5−10 ns) were performed using the GROMOS simulation package in conjunction with the GROMOS 53A6 force field taking the structure deposited within the protein data bank as the initial conformation.[11,12] The parameters for the fragments were generated using the Automated Topology Builder (ATB) and are available from the ATB repository (http://compbio.biosci.uq.edu.au/atb).[13] All of the 12 fragments identified by Drinkwater et al.[9] contain at least one 5- or one 6-membered aromatic ring. In the structures of the complexes deposited in the PDB, this ring lies sandwiched between the side chains of Phe182 and Asn39 forming a $\pi-\pi$ stacking interaction with the side chain of Phe182. In 9 out of 12 cases examined, the simulations confirmed that the fragment was stable in the proposed orientation with the root mean squared positional deviation (rmsd) of the fragment as compared to the X-ray structure ranging from 0.01 to 0.04 nm. In two cases, the fragment adopted a different orientation during the simulations. In the case of fragment 2 of cocktail 5 (**F2:5**; 4-bromoimadazole), the fragment adopted multiple binding modes. In contrast, in the case of **F1:11** (6-aminoquinoline), the fragment rotated by approximately 90° along the long axis of the fused ring relative to the binding mode proposed in the PDB 3KQP. In both cases, however, the position of the molecule within the binding pocket appeared to be compatible with the experimentally derived electron density. The simulations would thus support the proposal that these 11 fragments did indeed bind stably to PNMT. This is important as the binding of two fragments, **F4:8** (formanilide) and **F4:11** (2-hydroxynicotinic acid), could not be validated using ITC.

Only in one case, **F3:4** (6-chlorooxindole), was it not possible to reproduce the proposed binding mode in the simulations. Drinkwater et al.[9] proposed that 6-chlorooxindole adopted a unique binding mode. On the basis of fitting the compound within the experimentally derived electron density, they proposed that the fragment was stabilized solely by $\pi-\pi$ stacking interactions with the side chain of Phe182. No other stabilizing interactions such as specific hydrogen bonds or favorable dipole−dipole interactions were evident. The binding of **F3:4** could not be validated by ITC. In this case, the potential interaction of the other fragments in the cocktail was not examined explicitly. The volume of the density observed within the pocket was such that the assignment of the density to 6-chlorooxindole was considered unambiguous and the cocktail not deconvoluted (J. Martin, personal communication). To validate the proposed structure, multiple simulations were initiated from both the proposed X-ray structure as well as a variety of alternative binding modes. Irrespective of the initial placement of the fragment, **F3:4** was ejected from the binding pocket of PNMT within 50−100 ps of simulation. This strongly suggests that fragment **F3:4** does not bind stably to hPNMT.

If **F3:4** does not bind to hPNMT the question becomes what might account for the density observed experimentally. The four fragments contained in cocktail 4 are shown in Figure 2. As

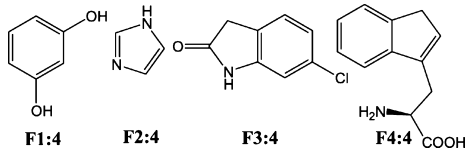

Figure 2. Four fragments of cocktail 4.

noted above PNMT catalyzes the conversion of *R*-noradrenaline to *R*-adrenaline (Figure 1). Noradrenaline and adrenaline both contain a benzene-1,2-diol group with a $-CH_2OH$ at position 4. Fragment **F1:4** is benzene-1,3-diol (resorcinol, Figure 2). A $-CH_nOH$ can often form similar interactions to −OH, and in this respect, benzene-1,3-diol might be considered a bioisostere of noradrenaline. Given this, it is conceivable that **F1:4** could bind to hPNMT. Fragment **F2:4** is imidazole. One of the 12 fragments identified by Drinkwater et al.[9] was 4-bromoimidazole (**F2:5**; PDB 3KQM) with a binding affinity of measured by ITC to be 170 μM. Thus, **F2:4** might also bind to PNMT.

To test whether fragment **F1:4** (resorcinol), **F2:4** (imidazole), or **F4:4** [(*S*)-3-(1*H*-inden-3-yl)-2-methylpropanoic acid] could bind stably to hPNMT and account for the observed density, a series of 5 ns simulations were performed in which each of the fragments in turn was placed within the binding pocket. Fragment **F1:4** adopted a stable binding mode irrespective of its initial placement in the pocket. The primary binding mode adopted by **F1:4** is shown in Figure 3a. The binding mode of noradrenaline determined crystallograpically is shown in Figure 3b. Clearly, the binding modes are very similar. Fragment **F2:4** (imidazole) remained in the pocket but like **F2:5** adopted a series of alternative binding modes during the simulation. The placement of **F4:4** in the binding pocket led to steric clashes, and clearly, **F4:4** does not bind to PNMT.

dx.doi.org/10.1021/ml300015u | *ACS Med. Chem. Lett.* 2012, 3, 322−326

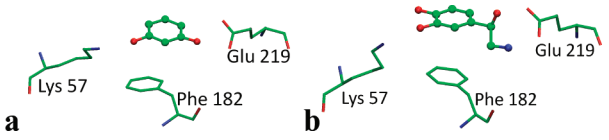

Figure 3. (a) Binding mode of fragment **F1:4** (ball and stick) to PNMT observed in MD simulation. (b) Binding mode of PNMT substrate noradrenaline (ball and stick) in the crystal structure 3HCD.

If fragments **F1:4** and **F2:4** form stable interactions with hPNMT, the question is whether they could individually explain the density observed experimentally. To investigate this, the electron density map was reanalyzed using the structure factors and atomic coordinates of the protein given in PDB 3KPY. Figure 4 shows the electron density map calculated as

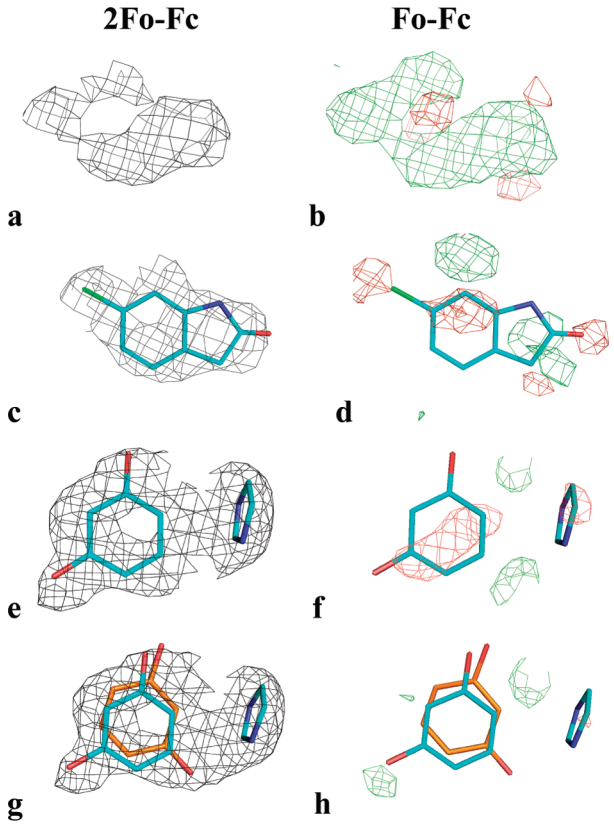

Figure 4. Electron density maps for PDB 3KPY (chain A) refined without any fragment (a and b), in the presence of fragment **F3:4** (c and d), in the presence of fragments **F1:4** and **F2:4** (e and f), and in the presence of **F2:4** and two binding modes of **F1:4** (cyan and orange), each with partial occupancies (g and h). $2F_o - F_c$ maps (black) are contoured at the 1.0σ level. $F_o - F_c$ maps are contoured at the +3.0σ level (positive "green" density) and −3.0σ level (negative "red" density).

$2F_o - F_c$ (contoured at 1.0σ) and as $F_o - F_c$ (contoured at +3.0σ green/positive and −3.0σ red/negative) for chain A of the PDB 3KPY. The equivalent electron density maps for chain B of the PDB 3KPY are given as Supporting Information (Figure S1). In Figure 4a,b, the electron density maps of the binding pocket correspond to the data as deposited in PDB 3KPY in the absence of any ligand. In the $F_o - F_c$ map, the green (positive) density indicates positions with excess density as compared to the structural model (i.e., positions where the placement of additional atoms is favored), while the red (negative) density indicates regions in which the density implied by the structural model is in excess of that suggested by the experimental data. The electron density maps for PDB 3KPY (with **F3:4**) are shown in Figure 4c,d. Although **F3:4** can account for the density in the $2F_o - F_c$ map (Figure 4c), the $F_o - F_c$ map (Figure 4d) shows significant regions of red (negative) density within the volume occupied by the ligand. There is also a significant volume of green (positive) density directly above the ligand in the region projecting toward Asp267. From Figure 4a,b, it is clear that **F1:4** and **F2:4** can be placed in multiple locations within the electron density and that in isolation they could not account for the volume of density observed. However, from the MD simulations, it was apparent that fragments **F1:4** and **F2:4** predominately occupy separate locations within the binding pocket. In particular, while **F1:4** primarily interacts with Phe182, **F2:4** adopted multiple binding modes binding primarily in a region close to Lys57. This suggests that **F1:4** and **F2:4** might bind simultaneously. A series of simulations were therefore performed in which **F1:4** and **F2:4** were placed together in the pocket.

In these simulations, fragment **F1:4** formed a $\pi-\pi$ stacking interaction with Phe182, one of the two −OH groups of **F1:4** formed a H-bond with the side chains of Asp267, while the other −OH group formed interactions with either Glu219 or projected toward **F2:4**. In the presence of **F1:4**, **F2:4** was restricted to a narrow range of binding modes and primarily lay perpendicular to the plane of **F1:4** close to Lys57. To determine if together these fragments could account for the diffraction data obtained experimentally, the structure 3KPY was rerefined using the original structure factors but with both **F1:4** and **F2:4** placed in the pocket. The rerefined density is shown in Figure 4e,f for the predominant orientation of **F1:4**. As can be seen, together, these fragments can account for all of the electron density in the binding pocket (Figure 4e). However, the $F_o - F_c$ map (Figure 4f) still shows significant negative (red) density over **F1:4** and positive (green) density at position C5 of **F1:4**. All alternate orientations of **F1:4** resulted in significant negative (red) density over the aromatic ring. In the MD simulations, **F1:4** adopted primarily two alternate orientations. Therefore, the structure was rerefined including two copies of **F1:4**, each with a partial occupancy. The resulting electron density maps are shown in Figure 4g,h. The $F_o - F_c$ map (Figure 4h) now shows no negative (red) density. The two alternate orientations of **F1:4** together were assigned ∼80% occupancy (cyan 50% and orange 30%, Figure 4h). The small regions of green (positive) density suggest that a third orientation of **F1:4** might also contribute to the observed density. Figure 4 clearly highlights the difficulty of using X-ray crystallography alone to determine the specific fragment, the correct binding mode, and even whether multiple ligands are present.

Although it is possible for **F1:4** and **F2:4** to occupy the binding pocket simultaneously, the critical question from a design perspective is whether the binding is cooperative. That is, would linking these two fragments lead to enhanced binding? To assess the degree the binding of **F1:4** and **F2:4** was cooperative, the difference in free enthalpy between the binding of **F1:4** and **F2:4** in isolation and the **F1:4** and **F2:4** together was calculated using the thermodynamic integration approach.[14] The net change in binding free enthalpy corresponding to the difference between the removal of a specific fragment free in solution and bound to the protein ($\Delta\Delta G$) is depicted in Figure 5. The thermodynamic cycle closes to within 2 kJ mol^{-1}, demonstrating that the calculations are well converged. It is also

dx.doi.org/10.1021/ml300015u | ACS Med. Chem. Lett. 2012, 3, 322−326

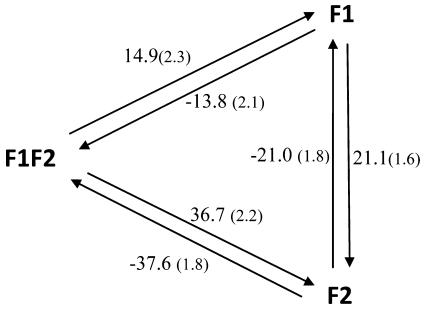

Figure 5. Relative free energy of binding (kJ mol^{-1}) for multiple fragments (**F1:4** and **F2:4**) binding to the protein phenylethanolamine *N*-methyltransferase (PNMT). The errors shown in parentheses were calculated by the formula $[(s_1)^2 + (s_2)^2]^{1/2}$, where s_1 and s_2 are the standard errors for the mutations in water and PNMT.

evident from Figure 5 that **F1:4** binds more tightly than **F2:4** by almost 21 kJ mol^{-1} but that the combination of **F1:4** and **F2:4** is more stable than either fragment **F1:4** or **F2:4** individually by 14 kJ mol^{-1}. In short, the binding is predicted to be highly cooperative.

Although together **F1:4** and **F2:4** can account for the density observed when the crystal was soaked using the cocktail, it is uncertain if they would be detected when soaked individually. As the binding of **F1:4** and **F2:4** is highly cooperative, it is likely that cocktail 4 would have appeared to be a false positive if deconvoluted. More than 25% of the hits obtained by Drinkwater et al.[9] in the initial crystallographic screens were considered to be false positives. That is, it was not possible to identify an individual fragment that could account for the density observed. The cocktails of fragments corresponding to the false positives are given in Table S1 in the Supporting Information. Structure factors are unavailable for these cases, and it is not possible to analyze if the density observed could be due to cooperative binding of more than one compound. Nevertheless, simulations of combinations of fragments in three of the cocktails (12, 13, and 14) were performed to examine if cooperativity might explain why these appeared as false positives. Individually, fragments **F1:12** (*p*-toluidine), **F2:12** (2-aminothiazole), **F1:13** (2-hydroxypyridine), **F4:13** (cyclohexan-1,4-dione), **F1:14** (2-aminopyrimidine), and **F4:14** [(1*R*,2*R*)-cyclohexane-1,2-diol] remained in the binding pocket for >5 ns, suggesting that they may bind weakly. These fragments were, however, highly mobile, and it is questionable if individually they would be detected crystallographically. In contrast, the combination of the two fragments from a given cocktail **F1:12** and **F2:12**, **F1:13** and **F4:13**, and **F1:14** and **F4:14** led to the formation of tertiary complexes that were stable on a 5 ns time scale. Representative configurations are provided in Figure S2 in the Supporting Information.

Crystallographic identification of fragments has many advantages in FBDD. However, as noted by others, current crystallographic protocols rarely lead to the direct identification of fragments that can be linked.[15,16] This is in part because these protocols are not tailored to finding tertiary complexes containing multiple fragments that bind cooperatively. The reasons for this are clear. The correct identification and determination of the binding mode of an isolated low molecular weight ligand based solely on medium to low-resolution X-ray data are challenging.[17] The problems are only compounded by the use of cocktails of molecules that individually bind only weakly. When deconvolution is not possible, valuable data are disregarded as noise or false positives. What has been illustrated here is that computational approaches can be used to overcome these hurdles. MD simulations and FE calculations can be used to identify stable tertiary complexes allowing crystallographic data from cocktails to be exploited. Finally, we would note that our simple analysis suggests that 4 of the 15 cocktails initially identified contained two compounds that bound cooperatively. How many alternative combinations might be found if cocktails containing different sets of these same fragments were investigated is an open question. What is clear, however, is that cases where combinations of fragment bind cooperatively and that are central to the fragment based approach are being missed.

■ ASSOCIATED CONTENT

Ⓢ Supporting Information

Details of the fragment cocktails, computational approach, and additional figures. This material is available free of charge via the Internet at http://pubs.acs.org.

Accession Codes

Coordinates and structure factors of rerefined PNMT complexed with **F1:4** (resorcinol, RCO), **F2:4** (imidazole, IMD), and AdoHcy (*S*-adenosyl-L-homocysteine, SAH) are available from the Protein Data Bank with accession code 4DM3.

■ AUTHOR INFORMATION

Corresponding Author

*Tel: +61 7 3365 4180. E-mail: a.e.mark@uq.edu.au.

Funding

Australian government and the University of Queensland for Endeavor International Postgraduate Research Scholarship (IPRS) to P.C.N. Australian Research Council (ARC; Grant No. DP 0987043) for the award of an Australian Post-Doctoral (APD) fellowship to A.K.M.

Notes

The authors declare no competing financial interest.

■ ACKNOWLEDGMENTS

We thank Prof. Jennifer L. Martin for providing access to the original data obtained during screening and for helpful discussions. We also thank Prof. Brett Collins for helpful discussions and Daniel Feder for helping during X-ray refinement. Computational resources were provided by the National Computational Infrastructure (NCI, Australia) projects m72 and n63.

■ REFERENCES

(1) Murray, C. W.; Rees, D. C. The rise of fragment-based drug discovery. *Nat. Chem.* **2009**, *1*, 187−192.

(2) Howard, N.; Abell, C.; Blakemore, W.; Chessari, G.; Congreve, M.; Howard, S.; Jhoti, H.; Murray, C. W.; Seavers, L. C. A.; van Montfort, R. L. M. Application of Fragment Screening and Fragment Linking to the Discovery of Novel Thrombin Inhibitors. *J. Med. Chem.* **2006**, *49*, 1346−1355.

(3) Geschwindner, S.; Olsson, L.-L.; Albert, J. S.; Deinum, J.; Edwards, P. D.; de Beer, T.; Folmer, R. H. A. Discovery of a Novel Warhead against β-Secretase through Fragment-Based Lead Generation. *J. Med. Chem.* **2007**, *50*, 5903−5911.

(4) Caldwell, J. J.; Davies, T. G.; Donald, A.; McHardy, T.; Rowlands, M. G.; Aherne, G. W.; Hunter, L. K.; Taylor, K.; Ruddle, R.; Raynaud, F. I.; Verdonk, M.; Workman, P.; Garrett, M. D.; Collins, I. Identification of 4-(4-Aminopiperidin-1-yl)-7H-pyrrolo[2,3-d]-pyrimidines as Selective Inhibitors of Protein Kinase B through Fragment Elaboration. *J. Med. Chem.* **2008**, *51*, 2147−2157.

(5) Chessari, G.; Woodhead, A. J. From fragment to clinical candidate—A historical perspective. *Drug Discovery Today* **2009**, *14*, 668−675.
(6) Congreve, M.; Chessari, G.; Tisi, D.; Woodhead, A. J. Recent Developments in Fragment-Based Drug Discovery. *J. Med. Chem.* **2008**, *51*, 3661−3680.
(7) Schulz, M. N.; Hubbard, R. E. Recent progress in fragment-based lead discovery. *Curr. Opin. Pharmacol.* **2009**, *9*, 615−621.
(8) Wyatt, P. G.; Woodhead, A. J.; Berdini, V.; Boulstridge, J. A.; Carr, M. G.; Cross, D. M.; Davis, D. J.; Devine, L. A.; Early, T. R.; Feltell, R. E.; Lewis, E. J.; McMenamin, R. L.; Navarro, E. F.; O'Brien, M. A.; O'Reilly, M.; Reule, M.; Saxty, G.; Seavers, L. C. A.; Smith, D.-M.; Squires, M. S.; Trewartha, G.; Walker, M. T.; Woolford, A. J. A. Identification of *N*-(4-Piperidinyl)-4-(2,6-dichlorobenzoylamino)-1*H*-pyrazole-3-carboxamide (AT7519), a Novel Cyclin Dependent Kinase Inhibitor Using Fragment-Based X-Ray Crystallography and Structure Based Drug Design. *J. Med. Chem.* **2008**, *51*, 4986−4999.
(9) Drinkwater, N.; Vu, H.; Lovell, K. M.; Criscione, K. R.; Collins, B. M.; Prisinzano, T. E.; Poulsen, S. A.; McLeish, M. J.; Grunewald, G. L.; Martin, J. L. Fragment-based screening by X-ray crystallography, MS and isothermal titration calorimetry to identify PNMT (phenylethanolamine N-methyltransferase) inhibitors. *Biochem. J.* **2010**, *431*, 51−61.
(10) Nair, P. C.; Malde, A. K.; Mark, A. E. Using Theory to Reconcile Experiment: The Structural and Thermodynamic Basis of Ligand Recognition by Phenylethanolamine N-Methyltransferase (PNMT). *J. Chem. Theory Comput.* **2011**, *7*, 1458−1468.
(11) Christen, M.; Hünenberger, P. H.; Bakowies, D.; Baron, R.; Bürgi, R.; Geerke, D. P.; Heinz, T. N.; Kastenholz, M. A.; Kräutler, V.; Oostenbrink, C.; Peter, C.; Trzesniak, D.; van Gunsteren, W. F. The GROMOS software for biomolecular simulation: GROMOS05. *J. Comput. Chem.* **2005**, *26*, 1719−1751.
(12) Oostenbrink, C.; Villa, A.; Mark, A. E.; van Gunsteren, W. F. A biomolecular force field based on the free enthalpy of hydration and solvation: The GROMOS force-field parameter sets 53A5 and 53A6. *J. Comput. Chem.* **2004**, *25*, 1656−1676.
(13) Malde, A. K.; Zuo, L.; Breeze, M.; Stroet, M.; Poger, D.; Nair, P. C.; Oostenbrink, C.; Mark, A. E. An Automated force field Topology Builder (ATB) and repository: Version 1.0. *J. Chem. Theory Comput.* **2011**, *7*, 4026−4037.
(14) Mark, A. E. Free energy perturbation calculations. In *Encyclopedia of Computational Chemistry 2*; von Rague Schleyer, P., Ed.; John Wiley & Sons: New York, 1998; pp 1070−1083.
(15) Sun, C.; Petros, A.; Hajduk, P. Fragment-based lead discovery: Challenges and opportunities. *J. Comput.-Aided Mol. Des.* **2011**, *25*, 607−610.
(16) Huth, J. R.; Park, C.; Petros, A. M.; Kunzer, A. R.; Wendt, M. D.; Wang, X.; Lynch, C. L.; Mack, J. C.; Swift, K. M.; Judge, R. A.; Chen, J.; Richardson, P. L.; Jin, S.; Tahir, S. K.; Matayoshi, E. D.; Dorwin, S. A.; Ladror, U. S.; Severin, J. M.; Walter, K. A.; Bartley, D. M.; Fesik, S. W.; Elmore, S. W.; Hajduk, P. J. Discovery and Design of Novel HSP90 Inhibitors Using Multiple Fragment-based Design Strategies. *Chem. Biol. Drug Des.* **2007**, *70*, 1−12.
(17) Malde, A. K.; Mark, A. E. Challenges in the determination of the binding modes of non-standard ligands in X-ray crystal complexes. *J. Comput.-Aided Mol. Des.* **2011**, *25*, 1−12.